

Physical impact of a surfactant on the nonlinear oscillations of a microbubble considering a dynamic surface tension and subject to an external acoustic field

C. Yepez , J. Naude ,* and F. Méndez *Departamento de Termodinámicos, Facultad de Ingeniería, Universidad Nacional Autónoma de México, 04510 CDMX, Mexico*

(Received 29 September 2021; accepted 18 May 2022; published 27 June 2022)

The dynamics of microbubbles under the action of external acoustic forces has become particularly important in several applications. In this work, we are particularly interested in studying the transport of surfactant molecules to the surface of an oscillating microbubble, considering the impact that the dynamic surface tension and temporal evolution of the radius of the microbubble has when an acoustic pressure as a driving force is used to promote the nonlinear oscillations. The resulting governing equations to predict the radius of the microbubble and the evolution of the surfactant at the surface are written in dimensionless form. For these equations, we identify two fundamental dimensionless parameters: the Gibbs elasticity E , and the cohesive (or repulsive) parameter K . Using the physical domain $0 \leq E \leq 10$ and $-13.2 \leq K \leq 13.2$, and considering that the diffusive Péclet number is large, as occurs in some applications, the surfactant concentration equation is solvable by using a similarity transformation, whereas the Rayleigh-Plesset-type equation that includes the influence of the previous parameters E and K is solved by the fourth-order Runge-Kutta method. When the numerical predictions are compared with the well-known cases $E = K = 0$, strong deviations reveal that the oscillation mechanisms can be significantly altered.

DOI: [10.1103/PhysRevFluids.7.063603](https://doi.org/10.1103/PhysRevFluids.7.063603)

I. INTRODUCTION

As is well known, the bubble dynamics is governed by the Rayleigh-Plesset equation (RP), a second-order nonlinear ordinary differential equation describing the response of a spherical bubble to a time-varying far-field pressure and originally developed by Lord Rayleigh in 1917, who studied the collapse of vapor cavities (free bubbles) to emulate the erosion of ship propellers [1,2] and modified by Plesset and other researchers in later work to account for the compressibility of the medium and other phenomena [3].

In contrast with a pure liquid, where the behavior of the microbubble is characterized by its initial size and properties of the surrounding liquid, in many applications, the presence of substances like surfactants, incorporated deliberately or that are founded in natural form, can easily adsorb at the interface forming a thin coating that affects the dynamic response and stability of the bubble by greatly reducing surface tension [4,5]. A surfactant molecule consists, in general, of a hydrophobic and a hydrophilic portion; because of this, surfactants tend to accumulate preferentially at the gas-liquid interfaces or to form new structures called micelles, when the critical micellar concentration (CMC) is reached [6]. There are two basic mechanisms by which the surfactant can come to the interface: using diffusive transport and considering the adsorption or kinetic transport in the neighborhood of the surface. The two of them compete to reach the equilibrium value for the surface concentration

*jorge_naude@hotmail.com

[7]. These extended models for which the influence of the surfactants is indispensable to understand the dynamics of the microbubble can be utilized to deduce other mechanisms that are present in the dynamic study of the nonlinear oscillations of the microbubbles [8–11]. On the other hand, in some industrial applications, the use of microbubbles with diameters between 1 and 100 μm serves to reach high gas dissolution rates or increase the adsorption performance. For these reasons, we consider it necessary to incorporate those physical-chemical aspects of the surfactants that can alter the different scenarios of the microbubble dynamics.

Considering the previous comments, the dynamics of encapsulated bubbles can be better understood if the presence of the surfactant is taken into account [2,12,13]. Along this line, Marmottant and co-workers included the transport of surfactant from the bulk phase to the interface and introduced a linear viscoelastic model with radius-dependent “ad hoc” effective surface tension [14]. Some recent studies have focused on replacing the ad hoc surface tension law in their model with a precise definition to avoid nonphysical transitions from one regime to the other. Most of the models mentioned do not take into account the effect of changes in the concentration of coating molecules adsorbed onto the bubble surface. Therefore, it is important to take this into account because experiments have shown that surfactant concentration has a considerable influence on some properties of the microbubble, particularly the surface tension [4,10,15].

Along this line of investigation, O’Brien *et al.* [16] and Fyrrillas and Szeri [6] dealt with the problem of surfactant transport and gas diffusion from and to the bubble. The latter used a complex splitting technique with a large Péclet number and concluded that the radius has a little variation with surfactant surface concentration; however, they did not relate the RP equation with the transport problem [6]. O’Brien, in turn, modified Marmottant’s model establishing the surface tension as a function of surface concentration and studied the effect of change in the bubble size distribution and coating properties using a pulse train on a bubble suspension. Their numerical analysis consisted in solving the wave equation coupled to a Rayleigh-Plesset equation in an iteration process in time and space for each bubble distribution in addition to solving a diffusion equation for gas and surfactant [16].

In this work, considering the previous comments, we study the influence that the surfactant surface concentration has on the radius of the microbubble, through a change in surface tension coupling the RP equation with the convection-diffusion equation for the surfactant transport together with proper boundary conditions. We identify that the diffusive Péclet number is large; therefore, the surfactant concentration equation can be decoupled from the Rayleigh-Plesset-type equation and solved in a closed form by using a similarity transformation. In addition, the model used to characterize the dynamic surface tension permits us to introduce two dimensionless parameters, E and K , which are directly related to the behavior of the interface. The above permits us to identify a boundary layer problem, in such a manner that we can introduce a proper change of coordinate to account for this, which immobilizes the interface and reduces the problem to an ordinary differential equation which is sufficient to predict the surfactant concentration.

II. PHYSICAL FORMULATION AND GOVERNING EQUATIONS

The problem consists of a single spherical microbubble with an initial radius of the order of micrometers, which is oscillating under the action of an external acoustic pressure field as can be seen in Fig. 1(a). In addition, the microbubble is filled with gas and immersed in an unbounded Newtonian incompressible fluid (for other media see Ref. [17]). The Newtonian fluid is used because the bubble radius and surfactant molecule size are small; then the non-Newtonian effects of biological fluids such as blood do not act on this scale [4].

To simplify the problem some assumptions must be made: The motion always remains spherically symmetric; the shell material is Newtonian; the interface is a zero-thickness model [13], which conforms to a monolayer encapsulating the bubble; and the bulk concentration is under the critical micellar concentration (CMC)—this latter to avoid the formation of new structures which could affect the studied problem.

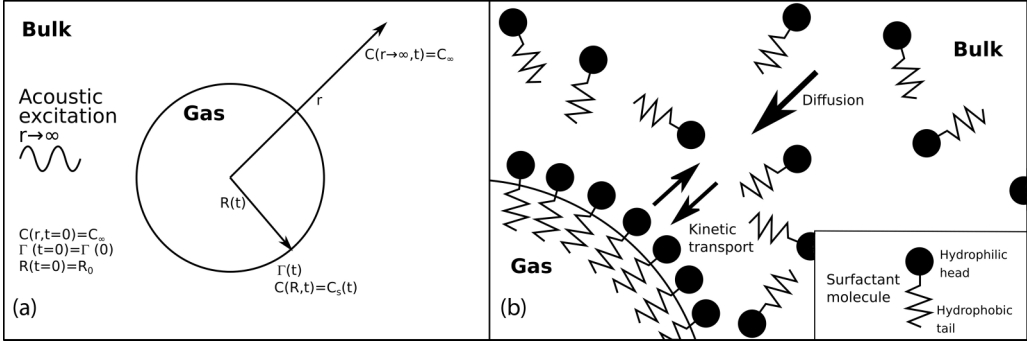


FIG. 1. (a) Schematic sketch of an encapsulated bubble with surfactant molecules under an acoustic excitation, with the initial and boundary conditions. (b) Close-up of the wall of the encapsulation, composed of a monolayer of surfactant molecules and considering a zero thickness because of the difference of magnitude between the radius of the bubble and the molecule size.

A. Governing equations

The Rayleigh-Plesset equation is used to model the change in the bubble radius under the presence of a prescribed ultrasound field, characterized by the angular frequency ω and the amplitude of the excitation pressure p_A . The basic form of this equation for an encapsulated Newtonian shell is [2]

$$\rho_L \left(R\ddot{R} + \frac{3}{2}\dot{R}^2 \right) + p_0 + p_A \cos \omega t - p_{G0} \left(\frac{R_0}{R} \right)^{3\gamma} + \frac{4\mu_L \dot{R}}{R} + \frac{4\dot{R}k^s}{R^2} + \frac{2\sigma(t)}{R} = 0, \quad (1)$$

where R is the instantaneous radius of the spherical bubble, \dot{R} and \ddot{R} are the first- and second-order time derivatives of the bubble radius, ρ_L is the density of the surrounding liquid, μ_L is the liquid viscosity, p_0 is the ambient pressure, and k^s is the shell surface viscosity—a relevant parameter for encapsulated bubbles since it is the only way to characterize the wall material within this equation. p_{G0} is the initial gas pressure and γ is the polytropic exponent, assuming the gas obeys a polytropic law.

The surface tension σ is considered as a dynamic quantity or variable because the area of the surface of the microbubble is changing due to the continuous oscillations of the microbubble. Well-established correlations for the dynamic surface tension as a function of the surfactant concentration can be found elsewhere (see Refs. [18,19]). Therefore, in this form and according to Frumkin's equation of state the surface tension is represented by

$$\sigma(t) = \sigma(0) + R_G T \Gamma_\infty \left[\ln \left(1 - \frac{\Gamma}{\Gamma_\infty} \right) + \frac{K}{2} \left(\frac{\Gamma}{\Gamma_\infty} \right)^2 \right], \quad (2)$$

where R_G is the universal gas constant, T is the temperature, and Γ_∞ is the maximum surface concentration attainable by the surface of the microbubble depending on the dissolved chemical species. K represents a parameter that measures the interaction between adjacent molecules; for $K < 0$ the molecules acquire a repulsive behavior, while for $K > 0$, the molecules present a cohesive behavior. For the case of $K = 0$, we recover the Langmuir model [19]. This parameter can be described in term of the energy for desorption [7], according to $K = \frac{\partial E_{des}}{\partial \Gamma} (\Gamma = 0)$.

On the other hand, the surfactant transport problem requires a transport equation for the bulk and in the case of a spherical bubble undergoing radial oscillations this is the convection-diffusion equation [6,20], which is given as

$$\frac{\partial C}{\partial t} + \frac{R^2 \dot{R}}{r^2} \frac{\partial C}{\partial r} = D \left(\frac{\partial^2 C}{\partial r^2} + \frac{2}{r} \frac{\partial C}{\partial r} \right), \quad (3)$$

where C is the bulk concentration defined as the mass per unit volume and D is the molecular diffusivity of the surfactant.

The initial and far-field boundary conditions as $r \rightarrow \infty$ on the scale on the bubble radius are

$$\begin{aligned} R(t=0) = R_0, \quad \dot{R}(t=0) = 0, \quad C(r, t=0) = C_\infty, \quad \Gamma(t=0) = \Gamma_0, \quad \text{and} \\ C(r \rightarrow \infty, t) = C_\infty. \end{aligned} \quad (4)$$

The previous conditions are referred to as an initial bubble radius different from zero and a resting interface: a constant value for the surfactant concentration in equilibrium with its surrounding environment at time zero and far away from the bubble interface; and finally an initial surfactant surface concentration value whose will be explained further in the Results section.

The boundary condition at the interface ($r = R$) for the bulk concentration C is expressed as a relation for nonequilibrium partitioning of a soluble surfactant between interface and bulk [6]:

$$\frac{d\Gamma(t)}{dt} + 2\frac{\dot{R}(t)}{R(t)}\Gamma(t) = D\frac{\partial C}{\partial r}[r = R(t), t], \quad (5)$$

where Γ is a surface-excess concentration residing on the interface, defined as the mass of surfactant per unit area (see Refs. [19,20]). In this manner, Eq. (5) represents the boundary condition that reflects the physical importance of the changes of the area of the microbubble being directly related with the diffusive mechanism from the surface of the microbubble to the surrounded liquid, and this surface activity is controlled by the adsorption and desorption mechanisms at the surface of the microbubble. Therefore, we can write Eq. (5) (according to the Frumkin model) as

$$\frac{d\Gamma(t)}{dt} + 2\frac{\dot{R}(t)}{R(t)}\Gamma(t) = \beta\Gamma_\infty C[r = R(t), t] \left[1 - \frac{\Gamma}{\Gamma_\infty} \right] - \alpha \exp \left[-K \frac{\Gamma}{\Gamma_\infty} \right] \Gamma. \quad (6)$$

The right-hand term is a kinetic expression where β and α represent the constants of adsorption and desorption, respectively; this term must be equal to the diffusion expression in Eq. (5) to reach equilibrium, in such a manner that the surfactant material can reach the interface. When adsorption-desorption kinetics is instantaneous, the surfactant concentration remains in equilibrium with $\Gamma(t)$ and the transport is only controlled by a diffusive regime, while if diffusion is rapid compared with the sorption kinetics, transport is called kinetically, or adsorption/desorption controlled [7].

B. Nondimensional governing equations

The system of Eqs. (1)–(6) may be nondimensionalized choosing the following natural scales. The characteristic timescale is related to the angular frequency ω through the relationship $\frac{1}{\omega}$; as length scale, we take the initial bubble radius R_0 , the surface concentration is nondimensionalized using the maximum surface concentration Γ_∞ , and the bulk concentration by the initial value C_∞ , i.e.,

$$\tau = t\omega, \quad a = \frac{R}{R_0}, \quad \eta = \frac{r}{R_0}, \quad \psi^s = \frac{\Gamma}{\Gamma_\infty}, \quad \psi = \frac{C}{C_\infty}. \quad (7)$$

Using the above dimensionless variables, the dimensionless governing equations given previously can be written as

$$a\ddot{a} + \frac{3}{2}\dot{a}^2 + \beta_0 + \beta_A \cos \tau - \frac{\beta_G}{a^{3\gamma}} + 4\frac{1}{\text{Re}}\frac{\dot{a}}{a} + 4\delta\frac{\dot{a}}{a^2} + \frac{\text{We}}{a} \left\{ 1 + E \left[\ln(1 - \psi^s) + \frac{K}{2}(\psi^s)^2 \right] \right\} = 0, \quad (8)$$

where Re is the Reynolds number, δ represents the dimensionless shell viscosity, We is the Weber number, and finally E is the elasticity number or Gibbs elasticity and provides a measure of the sensitivity of surface tension to surface concentration.

The last term of the right-hand side of Eq. (8) is called the surface pressure [6] and for the Frumkin isotherm it has the following form:

$$\pi^* = E \left[\ln(1 - \psi^s) + \frac{K}{2} (\psi^s)^2 \right]. \quad (9)$$

We use this form because it is easy to see how surface tension is decreased with the presence of surfactant molecules on the interface and the relevance that the elasticity parameter E has.

On the other hand, the equation for the surfactant concentration can be written in dimensionless form as

$$\frac{\partial \psi}{\partial \tau} + \frac{a^2 \dot{a}}{\eta^2} \frac{\partial \psi}{\partial \eta} = \frac{1}{\text{Pe}} \left(\frac{\partial^2 \psi}{\partial \eta^2} + \frac{2}{\eta} \frac{\partial \psi}{\partial \eta} \right), \quad (10)$$

while from Eq. (5) we have

$$\frac{d\psi^s}{d\tau} + \frac{2\dot{a}}{a} \psi^s = J \frac{1}{\text{Pe}} \frac{\partial \psi}{\partial \eta} \Big|_{\eta=a}, \quad (11)$$

and the temporal evolution of the surfactant concentration in terms of the kinetics parameters can be written in dimensionless form as follows:

$$\begin{aligned} \frac{d\psi^s}{d\tau} + \frac{2\dot{a}}{a} \psi^s &= \beta^* \psi|_{\eta=a} (1 - \psi^s) - \alpha^* \psi^s \exp[-K\psi^s] \\ &= \alpha^* \{ P \psi|_{\eta=a} (1 - \psi^s) - \psi^s \exp[-K\psi^s] \}. \end{aligned} \quad (12)$$

In the set of Eqs. (8)–(12) appear the following dimensionless parameters:

$$\begin{aligned} \beta_G &= \frac{P_{G0}}{\rho_l R_0^2 \omega^2}, & \beta_A &= \frac{P_A}{\rho_l R_0^2 \omega^2}, & \beta_0 &= \frac{P_0}{\rho_l R_0^2 \omega^2}, & \delta &= \frac{k^s}{\rho_l R_0^3 \omega}, \\ \text{Pe} &= \frac{R_0^2 \omega}{D}, & \text{Re} &= \frac{\rho_l R_0^2 \omega}{\mu_l}, & \text{We} &= \frac{2\sigma_0}{\rho_l R_0^3 \omega^2}, & E &= \frac{R_G T \Gamma_\infty}{\sigma_0}, \\ \alpha^* &= \frac{\alpha}{\omega}, & \beta^* &= \frac{\beta C_\infty}{\omega}, & J &= \frac{C_\infty R_0}{\Gamma_\infty}, & P &= \frac{\beta C_\infty}{\alpha}. \end{aligned} \quad (13)$$

Due to the multiparametric nature of the resulting governing equations, here we are particularly interested in the asymptotic analysis of the governing equations dictated by the assumed values of some characteristic parameters. For instance, the Péclet number denoted by Pe , in practical cases, can assume large values because R_0 is of the order of $1 \mu\text{m}$, ω is of the order of $1 \times 10^7 \text{ Hz}$, and D is of the order of $1 \times 10^{-10} \text{ m}^2 \text{ s}^{-1}$ as can be seen in Table I. Therefore, in this case, Pe is larger than the unit, and a concentration boundary layer of the surfactant is developed in the external region next to the surface of the microbubble. In the following lines, we take advantage of this fact. On the other hand, J represents a dimensionless adsorption depth that measures the distance over which surfactant molecules must diffuse to supply the interface [7] and P is simply the ratio between adsorption and desorption coefficients. Finally, the rest of the boundary and initial conditions in dimensionless form can be written as

$$\begin{aligned} a(\tau = 0) &= 1, & \dot{a}(\tau = 0) &= 0, & \psi(\eta, \tau = 0) &= 1, \\ \psi^s(\tau = 0) &= \psi^s(0), & \text{and } \psi(\eta \rightarrow \infty, \tau) &= 1. \end{aligned} \quad (14)$$

TABLE I. Geometric and physical properties together with the values of the dimensionless parameters used in the present work and taken from Ref. [18].

Parameter	Value	Units	Dimensionless parameter	Value
R_0	1.00×10^{-6}	m	γ	1.4
$\omega = 2\pi f$	1.88×10^7	Hz	Re	18.85
P_A	4.00×10^5	Pa	β_A	1.126
P_0	101.3×10^3	Pa	β_0	0.285
P_{G0}	2.45×10^5	Pa	B_G	0.689
ρ_l	1000	kg m^{-3}	E	0.1897
μ_l	1.00×10^{-3}	Pa s	J	1.13×10^{-3}
σ_0	0.072	N m^{-1}	We	0.405
D	4.00×10^{-10}	$\text{m}^2 \text{s}^{-1}$	Pe	4.7×10^4
K^s	8.00×10^{-8}	N s m^{-1}	δ	4.244
B	5.6	$\text{m}^3 \text{mol}^{-1} \text{s}^{-1}$	β^*	1.78×10^{-9}
A	1.29×10^{-5}	S^{-1}	α^*	6.83×10^{-13}
Γ_∞	5.3×10^{-6}	mol m^{-2}	ψ^s_{eq}	0.99
C_∞	0.006	mol m^{-3}	P	2608.7

III. ASYMPTOTIC LIMIT $\text{Pe} \gg 1$

In this section, we use the similarity method [21] under the limit $\text{Pe} \gg 1$. The problem is characterized by a large Péclet number as was previously commented on in the last section. Physically, the rate at which the molecules of surfactant are populating the interface is limited by the slow transport, via the diffusive mechanism, which is presented between the liquid and the interface. This last mechanism is controlled by the adsorption and desorption capacities according to Eqs. (11) and (12) [6].

From a mathematical point of view with the aid of singular perturbation techniques [22], the limit of $\text{Pe} \gg 1$ represents a singular problem for Eq. (10), because in this case, the derivatives of higher order are multiplied by a small parameter; hence the problem must be treated at large but finite Pe . Therefore, in this limit a concentration boundary layer for the surfactant in a region near the surface of the microbubble can be studied with the aid of the following stretching variable:

$$\zeta = \frac{\eta - a(\tau)}{\varepsilon^2}, \quad (15)$$

where $\varepsilon = \text{Pe}^{-\frac{1}{2}}$ is the thickness of the boundary layer in terms of Péclet number. Substituting the stretching variable in Eq. (10) we have

$$\frac{\partial \psi}{\partial \tau} - \frac{1}{\varepsilon^2} \frac{\partial a}{\partial \tau} \frac{\partial \psi}{\partial \zeta} + \frac{a^2}{(a + \varepsilon^2 \zeta)^2} \frac{\partial a}{\partial \tau} \frac{1}{\varepsilon^2} \frac{\partial \psi}{\partial \zeta} = \frac{1}{\text{Pe}(a + \varepsilon^2 \zeta)^2} \frac{1}{\varepsilon^4} \frac{\partial}{\partial \zeta} \left[(a + \varepsilon^2 \zeta)^2 \frac{\partial \psi}{\partial \zeta} \right], \quad (16)$$

where the following term can be identified and rewritten as

$$\eta^2 = (a + \varepsilon^2 \zeta)^2 = a^2 \left(1 + \frac{\varepsilon^2 \zeta}{a} \right)^2, \quad (17)$$

and taking into account that $\frac{\varepsilon^2 \zeta}{a} \ll 1$; because of the large value of the Péclet number, then $a^2 \left(1 + \frac{\varepsilon^2 \zeta}{a} \right)^2 \approx a^2$, and Eq. (16) is simplified, resulting in

$$\varepsilon^2 \frac{\partial \psi}{\partial \tau} = \frac{\partial^2 \psi}{\partial \zeta^2}. \quad (18)$$

In this manner, the curvature terms are negligible, and the diffusion mechanism is decoupled from the oscillations of the microbubble. Now, introducing the similarity variable $\xi = \frac{\varepsilon\zeta}{2\sqrt{\tau}}$, we can transform Eq. (18) which represents converting a partial differential equation into a simple ordinary differential equation, which can be written as follows:

$$\frac{d^2\psi}{d\xi^2} = -2\xi \frac{d\psi}{d\xi}. \quad (19)$$

Integrating once,

$$\frac{d\psi}{d\xi} = C_1 \exp(-\xi^2), \quad (20)$$

Integrating again we have

$$\psi = C_1 \int_0^\infty \exp(-\xi^2) d\xi + C_2 = C_1 \frac{\sqrt{\pi}}{2} \operatorname{erf}(\xi) + C_2. \quad (21)$$

In the above expression, the symbol $\operatorname{erf}(\xi)$ represents the error function. To evaluate the constants of integration, it is necessary to consider the limit far away from the interface ($\eta \rightarrow \infty$, $\zeta \rightarrow \infty$, $\xi \rightarrow \infty$) from Eq. (14), and knowing that $\lim_{\xi \rightarrow \infty} \operatorname{erf}(\xi) = 1$, we have

$$1 = C_1 \frac{\sqrt{\pi}}{2} + C_2. \quad (22)$$

When using the initial condition ($\tau = 0$), it collapses in the same limit for $\xi \rightarrow \infty$, so it remains for us to use the expression for the boundary condition ($\xi = 0$), with which we have

$$\psi(0) = C_2, \quad C_1 = \frac{2}{\sqrt{\pi}} [1 - \psi(0)], \quad (23)$$

and substituting these constants in Eq. (21) the final form for the bulk concentration is obtained:

$$\psi = [1 - \psi(0)] \operatorname{erf}(\xi) + \psi(0). \quad (24)$$

With the aid of the above equation, we can easily obtain the derivative:

$$\frac{d\psi}{d\xi} = \frac{2}{\sqrt{\pi}} [1 - \psi(0)] \exp(-\xi^2). \quad (25)$$

Then this derivative can be directly replaced in Eq. (11), obtaining that

$$\frac{d\psi^s}{d\tau} + \frac{2\dot{a}}{a} \psi^s = \frac{J\varepsilon}{\sqrt{\pi\tau}} [1 - \psi(0)], \quad \tau > 0. \quad (26)$$

From the last expression, $\psi(0)$ can be obtained and substituted in Eq. (12) instead of $\psi|_{\eta=a}$, obtaining a differential equation for ψ^s as the only dependent variable:

$$\frac{d\psi^s}{d\tau} + \frac{2\dot{a}}{a} \psi^s = \frac{\beta^*(1 - \psi^s) - \alpha^* \psi^s \exp[-K\psi^s]}{1 + \beta^*(1 - \psi^s) \frac{\sqrt{\pi\tau}}{J\varepsilon}}. \quad (27)$$

Equation (27), together with the RP equation [Eq. (8)] and the rest of the boundary and initial conditions [Eq. (14)] constitutes a coupled system of ordinary differential equations for the radius and the surface concentration.

IV. RESULTS

Through Eqs. (8), (14), and (27) the radius and the surface concentration can be obtained, whereas the surface pressure term is acquired from Eq. (9). The system of Eqs. (8) and (27) can be

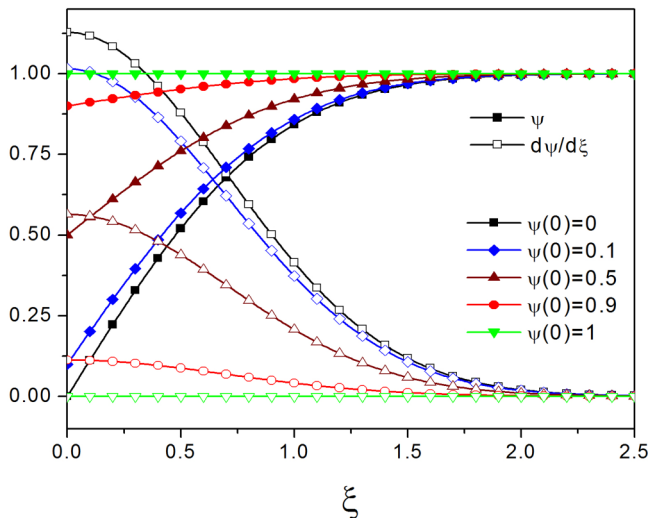


FIG. 2. The distribution of the dimensionless bulk surfactant concentration ψ and its derivative $\frac{d\psi}{d\xi}$ as a function of the dimensionless coordinate ξ , for five different values of the parameter $\psi(0)$, according to Eqs. (24) and (25).

easily solved with the aid of the fourth-order Runge-Kutta method if the following transformations are used:

$$R_1 = a, \quad R_2 = \frac{dR_1}{d\tau}. \quad (28)$$

The condition for the surfactant surface concentration can be supposed zero [$\psi^s(0) = 0$] if the microbubble is generated at the beginning of the phenomenon, or with an equilibrium value, which can be obtained if the bubble has reached this condition at a previous time [7]. Surface concentration in equilibrium can be easily obtained if the left-hand side of Eq. (12) is equal to zero, using $K = 0$ as in the Langmuir model and supposing that $\psi = 1$ (far away from the bulk concentration), and given the high value of P we have [7]

$$\psi_{\text{eq}}^s = \frac{P}{(P+1)} \approx 0.9. \quad (29)$$

Simulation parameters used in the present work are given in Table I. The liquid is taken as water at 310 K, while the values for β , α , D , C_∞ , and Γ_∞ are taken from [18] corresponding to a nonionic alkyl polyglycol ether surfactant, $C_{12}E_8$. The initial radius and pressure values are commonly found in ultrasound cavitation literature. Although mentioned before, we use the value $\psi^s(0) = 0.5$ for the set of figures presented here. This is because it is quite far away from the critical value $\psi^s = 1$ and shows a good amplitude range for the variables, unlike the value $\psi^s = 0$.

Figure 2 shows the behavior of ψ and $\frac{d\psi}{d\xi}$ as function of the dimensionless coordinate ξ for five different values of the dimensionless parameter $\psi(0)$. For this figure, the bulk concentration $\psi(\xi)$ has a boundary layer behavior that $\psi(0) \rightarrow 0$ always. Otherwise, the previous tendency disappears. On the other hand, the derivative of the bulk concentration $\frac{d\psi}{d\xi}$, that physically represents the existence of strong gradients, offers a trivial solution when $\psi(0) \rightarrow 0$, because in this last case, the concentration field is uniform for all values of the dimensionless coordinate ξ .

In Fig. 3, we show a comparison between the present model and Marmottant's model [14]. Here we see how the compressibility does not affect the radius of the bubble because the values of the parameters lead to a low Mach number ($M = 0.012$), a term present in the reference. And even when the base of each model is different (the parameter that leads to dynamic surface tension is

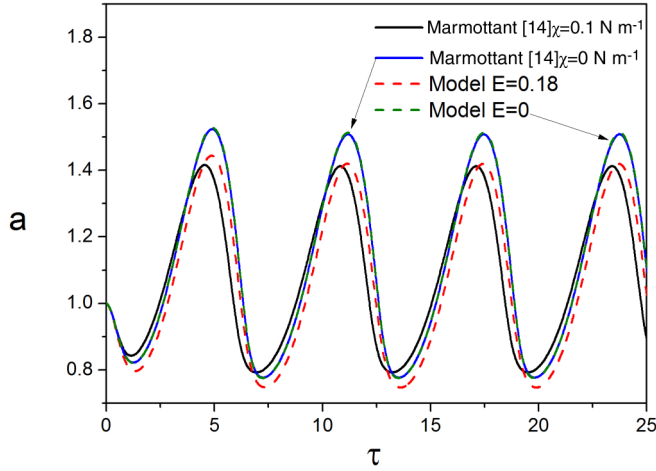


FIG. 3. Comparison between the model developed in this work and the Marmottant model [14]. Dimensionless radius a as a function of the dimensionless time τ for $\beta_0 = 0.321$, $\beta_A = 1.1257$, $\text{Re} = 17.322$, $\text{We} = 0.468$, and $\delta = 0.88$.

the so-called shell elasticity $\chi[\text{N m}^{-1}]$, for Marmottant, and the elasticity parameter E , for this work), the agreement between the two curves is good, and a direct comparison study between the parameters would be necessary.

In Fig. 4, we show the dimensionless radius a as a function of the dimensionless time τ for three different values of the parameter $\psi^s(0)$ ($= 0.2, 0.5$, and 0.7). The general behavior is oscillating around an equilibrium radius a , different from the initial value $a_0 = 1$; this can be estimated as the mean value after some cycles and is lower as $\psi^s(0)$ increases, keeping the amplitude. On the other hand, for the variables ψ^s and π^* , the amplitude is increased as seen in Figs. 5 and 6, respectively. ψ^s oscillates around the initial value of this distribution, while surface pressure π^* has similar behavior, given the direct dependence on surface concentration.

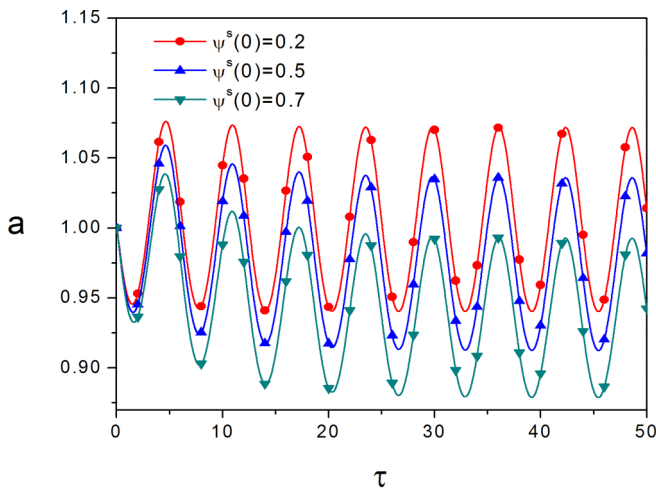


FIG. 4. Dimensionless radius a as a function of the dimensionless time τ for three different values of the initial surface concentration, $\psi^s(0)$, $\beta_A = 1.1257$, $E = 0.19$, $K = 13.2$, and $\delta = 4.244$.

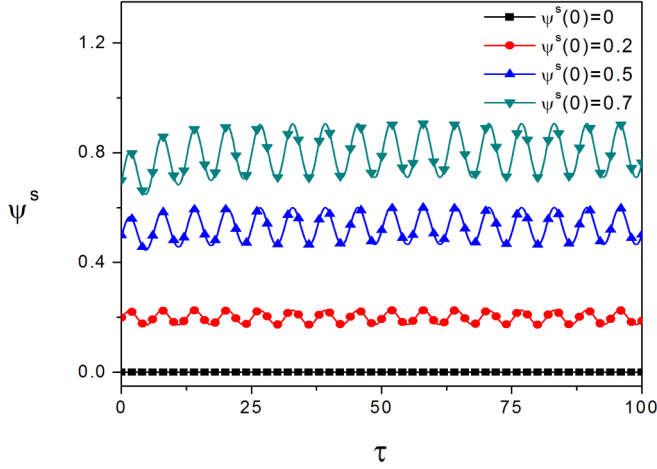


FIG. 5. Dimensionless surface concentration ψ^s as a function of the dimensionless time τ for four different values of the initial surface concentration, $\psi^s(0)$, $\beta_A = 1.1257$, $E = 0.19$, $K = 13.2$, and $\delta = 4.244$.

In Figs. 7 and 8, the dimensionless radius and the surface pressure are plotted as functions of the elasticity parameter E , respectively. With a higher value of E , the radius amplitude a is lower. Conversely ψ^s and π^* have a higher value and the amplitude increases. $E = 5$ seems to be a critical value for which the oscillations disappear for the used scale of the radius. However, making a close-up about $a \sim 0.708$, we can appreciate a weak oscillation around this value as shown in Fig. 7(b). Similar comments can be made for Fig. 8. For the case $E = 10$, the oscillations disappear completely, and a cavitation regime is established under these circumstances. For the surface concentration, the oscillation occurs under the critical limit $\psi^s = 1$. When $E > 5$ a value $\psi^s \geq 1$ is reached and the solution fails; physically it is impossible for the microbubble surface to hold this number of molecules, and mathematically the model cannot calculate data beyond these values. It should be noted that the value used in this work for the elasticity parameter is $E < 1$, so

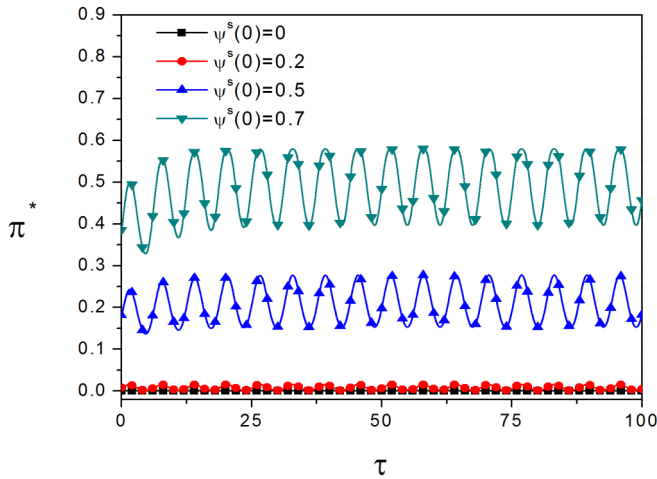


FIG. 6. Dimensionless surface pressure π^* as a function of the dimensionless time τ for four different values of the initial surface concentration, $\psi^s(0)$, $\beta_A = 1.1257$, $E = 0.19$, $K = 13.2$, and $\delta = 4.244$.

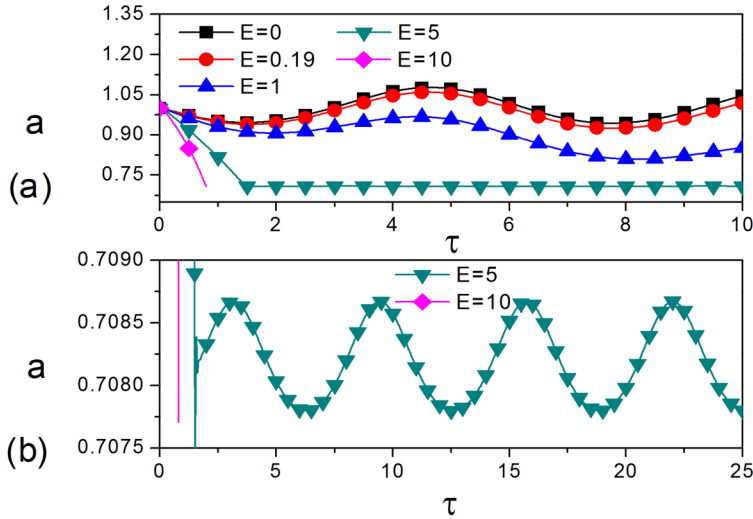


FIG. 7. (a) Dimensionless radius a versus the dimensionless time τ for five different values of the elasticity parameter E : $\psi^s(0) = 0.5$, $\beta_A = 1.1257$, $K = 13.2$, and $\delta = 4.244$. (b) Close-up, showing the oscillation for $E = 5$ around the bubble radius $a \approx 0.708$.

the other values are only used to see the general behavior of the variables with their variation; these include the extreme values $E = 0, 5, 10$.

In the next group of figures, we choose both positive and negative values for the molecular interaction parameter K to see the general behavior of the dependent variables, remembering the value depends on the surfactant specie. With $K > 0$, the radius has a negative displacement, reaching lower values, while surface pressure has a positive displacement, as seen in Figs. 9 and 10. On the other hand, with K negative the radius reaches higher levels, while with ψ^s the opposite happens. The amplitude range seems to be quite similar for all the cases, so the interaction between adjacent molecules only generates a displacement on the curves for the radius and the surface concentration and a slight increase on surface pressure amplitude as the magnitude of K increases.

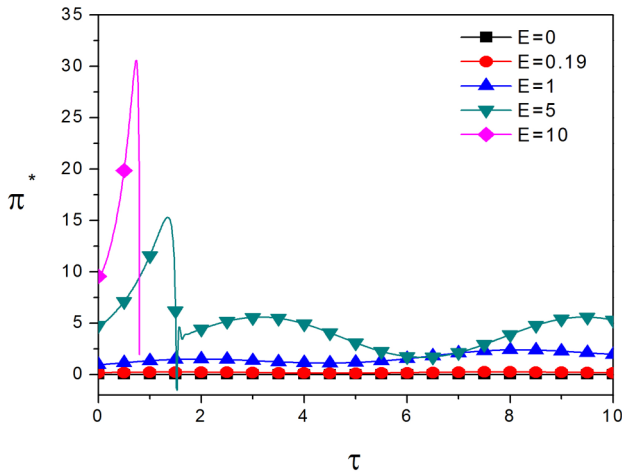


FIG. 8. Dimensionless surface pressure π^* versus the dimensionless time τ for five different values of the elasticity parameter E ; $\psi^s(0) = 0.5$, $\beta_A = 1.1257$, $K = 13.2$, and $\delta = 4.244$.

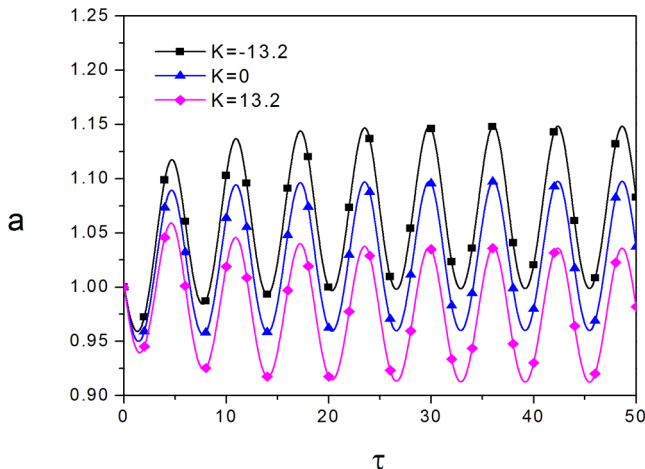


FIG. 9. Dimensionless radius a as a function of the dimensionless time τ for three different values of the molecular interaction parameter K : $\psi^s(0) = 0.5$, $\beta_A = 1.1257$, $E = 0.19$, and $\delta = 4.244$.

Figure 11 shows the trend of the mean value for the radius of the microbubble (a_{mean}) and the surface concentration (ψ_{mean}^s) with the relevant parameters shown above. We choose the “mean” values since they work as good indicators of the behavior of the variables when the oscillation becomes periodic. In Fig. 11 (lower), a linear behavior is seen for a_{mean} and ψ_{mean}^s , decreasing the value for the radius and increasing the mean values for the surface concentration as K increases. In Fig. 11 (upper), a_{mean} tends to decrease and reach an asymptotic value with E higher, while ψ_{mean}^s tends to grow with an asymptotic limit of $\psi_{\text{mean}}^s \approx 1$ for E .

V. CONCLUSIONS

The surfactant surface concentration is an important aspect in dealing with microbubbles in biological fluids; as noted, the natural or deliberated presence can be beneficial if one can

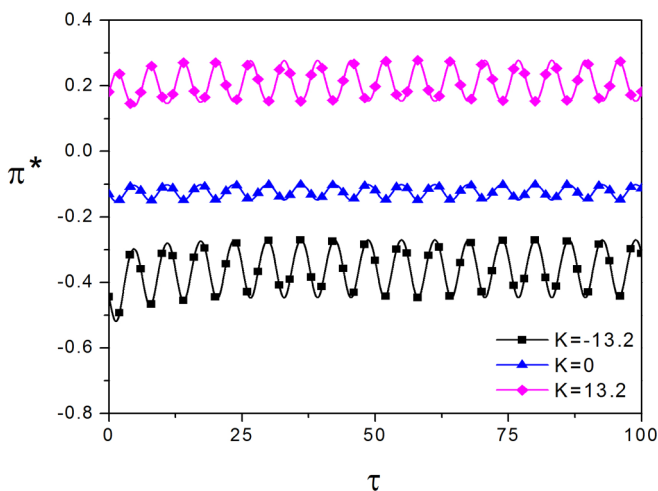


FIG. 10. Dimensionless surface concentration ψ^s as a function of the dimensionless time τ for three different values of the molecular interaction parameter K : $\psi^s(0) = 0.5$, $\beta_A = 1.1257$, $E = 0.19$, and $\delta = 4.244$.

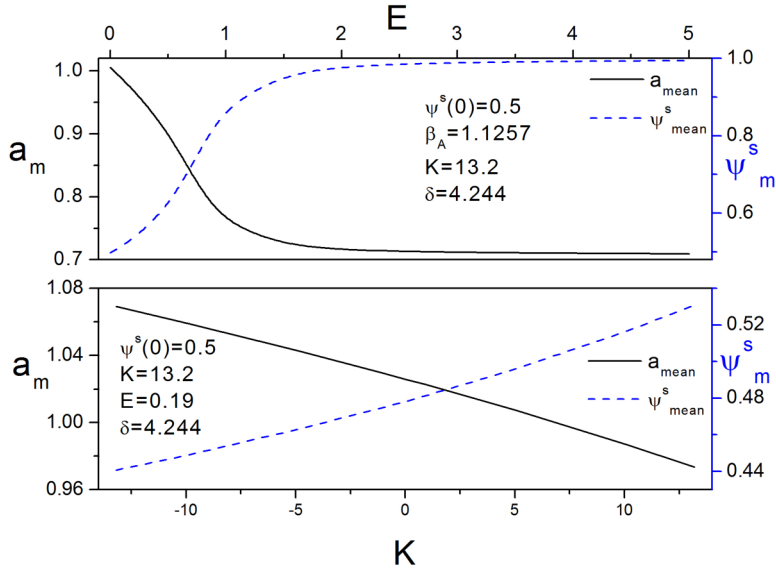


FIG. 11. Mean values of the dimensionless radius a_{mean} and the surface concentration ψ_{mean}^s as functions of (upper) the elasticity parameter E , and (lower) the molecular interaction parameter K , for $\psi^s(0) = 0.5$. The values of the rest of the parameters are indicated in each graphic.

understand and anticipate the behavior of the bubble. Parameters such as the driving force, the elasticity number, and dimensionless shell viscosity have great relevance in the bubble radius evolution and subsequently in surface concentration value through the change in surface tension that surfactant molecules generate. Therefore, there exists a strong relationship between the radius of the bubble and the surface concentration that must be considered and can be appreciated through the Results section, in which the radius oscillations and the surface concentration profiles are affected by each other. Our model, in contrast with others, includes such relationship, and a second equation for surfactant transport is necessary, which affects the traditional RP equation through the elasticity parameter and the molecular interaction parameter, strongly dependent on the chemical species, such as hydrodynamics, thermodynamics, and chemical properties of the phenomena.

The ultrasound amplitude and frequency are the parameters in which one has freedom of choice once the chemical species and fluid are set. Knowing the influence of these parameters may bring a better understanding of the phenomena and their application in areas such as medicine or new areas of interest.

The similarity method allows obtaining fast results when the Péclet number is high and there is a boundary layer, useful in this case given the characteristic values for the initial radius, the ultrasound frequency, and diffusion coefficient found in the acoustic dynamics of microbubbles. Eliminating the convection-diffusion equation through an appropriate coordinate shift gives an easier solving process that only involves the RP equation and the surface concentration evolution equation—a system that is solvable through a fourth-order Runge-Kutta method and without iterations like in other works.

The model obtained can be useful for other kinds of analyses such as multiple scales or even considering a non-Newtonian shell material, adding the proper stress-deformation relationship, because, at this point, we are dealing only with a first-order differential equation system.

For future work, it is possible to add surface concentration as a function of time and space, which can lead to movement of the molecules on the surface and Marangoni effects because of

the concentration gradient. Another area is the use of other types of driving pressure, for example, a pulse train or a Gaussian pulse, which would change the dynamic of the bubble and bring a panorama about the use of microbubbles as contrast agents.

ACKNOWLEDGMENTS

We would like to express thanks for the financial support from PAPIIT UNAM Project No. IN-108421. C.Y. would like to thank the Mexican National Council for Science and Technology (CONACYT) for the scholarship granted for the completion of his doctoral studies.

-
- [1] C. E. Brennen, *Cavitation and Bubble Dynamics* (Oxford University Press, Oxford, 1995), p. 48.
 - [2] S. Paul, R. Nahire, S. Mallik, and K. Sarkar, Encapsulated microbubbles and echogenic liposomes for contrast ultrasound imaging and targeted drug delivery, *Comput. Mech.* **53**, 413 (2014).
 - [3] A. Doinikov and A. Bouakaz, Review of shell models for contrast agent microbubbles, *IEEE Trans. Ultrason. Ferroelectr. Freq. Control* **58**, 981 (2011).
 - [4] E. Stride, The influence of surface adsorption on microbubble dynamics, *Philos. Trans. R. Soc. A* **366**, 2103 (2008).
 - [5] T. Faez, 20 Years of ultrasound contrast agent modeling, *IEEE Trans. Ultrason. Ferroelectr. Freq. Control* **60**, 7 (2013).
 - [6] M. M. Fyrrillas and A. J. Szeri, Surfactant dynamics and rectified diffusion of microbubbles, *J. Fluid Mech.* **311**, 361 (1996).
 - [7] F. Jin, R. Balasubramaniam, and K. J. Stebe, Surfactant adsorption to spherical particles: The intrinsic length scale governing the shift from diffusion to kinetic-controlled mass transfer, *J. Adhes.* **80**, 773 (2004).
 - [8] S.-T. Kang and C.-K. Yeh, Ultrasound microbubble contrast agents for diagnostic and therapeutic applications: Current status and future design, *Chang Gung Med J.* **35**, 125 (2012).
 - [9] M. Postema and A. Van Wamel, Ultrasound-induced encapsulated microbubble phenomena, *Ultrasound Med. Biol.* **30**, 827 (2004).
 - [10] K. Sarkar and W. T. Shi, Characterization of ultrasound contrast microbubbles using *in vitro* experiments and viscous and viscoelastic interface models for encapsulation, *J. Acoust. Soc. Am.* **118**, 539 (2005).
 - [11] Y. Liu, K. Sugiyama, S. Takagi, and Y. Matsumoto, Surface instability of an encapsulated bubble induced by an ultrasonic pressure wave, *J. Fluid Mech.* **691**, 315 (2012).
 - [12] C. C. Church, The effects of an elastic solid-surface layer on the radial pulsation of gas bubbles, *J. Acoust. Soc. Am.* **97**, 1510 (1995).
 - [13] N. de Jong, L. Hoff, T. Skotland, and N. Bom, Absorption and scatter of encapsulated gas filled microspheres: Theoretical consideration and some measurements, *Ultrasonics* **30**, 95 (1992).
 - [14] P. Marmottant, S. van der Meer, M. Emmer, M. Versluis N. de Jong, S. Hilgenfeldt, and D. Lohse, A model for large amplitude oscillations of coated bubbles accounting for buckling and rupture, *J. Acoust. Soc. Am.* **118**, 3499 (2005).
 - [15] J. P. O'Brien, N. Ovenden, and E. Stride, Accounting for the stability of microbubbles to multi-pulse excitation using a lipid-shedding, *J. Acoust. Soc. Am.* **130**, EL180 (2009).
 - [16] J. P. O'Brien, E. Stride, and N. Ovenden, Surfactant shedding and gas diffusion during pulsed ultrasound through a microbubble contrast agent suspension, *J. Acoust. Soc. Am.* **134**, 1416 (2013).
 - [17] M. T. Warnez and E. Johnsen, Numerical modeling of bubble dynamics in viscoelastic media with relaxation, *Phys. Fluids* **27**, 063103 (2015).
 - [18] N. J. Alvarez, L. M. Walker, and S. L. Anna, Diffusion-limited adsorption to a spherical geometry: The impact of curvature and competitive time scales, *Phys. Rev. E* **82**, 011604 (2010).
 - [19] L. G. Leal, *Advanced Transport Phenomena. Fluid Mechanics and Convective Transport Processes* (Cambridge University Press, New York, 2007).

- [20] D. A. Edwards, H. Brenner, and D. T. Wasan, *Interfacial Transport Processes and Rheology* (Butterworth-Heinemann, Boston, 1991).
- [21] C.-L. Ho and C.-C. Lee, Similarity solutions of reaction-diffusion equation with space- and time-dependent diffusion and reaction terms, [Ann. Phys. **364**, 148 \(2016\)](#).
- [22] C. M. Bender and S. A. Orszag, *Advanced Mathematical Methods for Scientists and Engineers. I. Asymptotic Methods and Perturbation Theory* (Springer, Berlin, 1999).